Int J Earth Sci (Geol Rundsch)
DOI 10.1007/s00531-013-0996-z

ORIGINAL PAPER

Geochronology and geochemistry of the Late Triassic Longtan pluton in South China: termination of the crustal melting and Indosinian orogenesis

Liang Qiu · Dan-Ping Yan · Mei-Fu Zhou · Nicholas T. Arndt · Shuang-Li Tang · Liang Qi

Received: 9 April 2013 / Accepted: 20 December 2013

Abstract The Indosinian orogeny is recorded by Triassic angular unconformities in Vietnam and South China and by widely occurring granitoids in the Yunkai-Nanling and the Xuefengshan belts of South China. The Longtan pluton in the northwestern part of the Xuefengshan belt is a typical high-K, calc-alkaline, I-type granitoid, which can shed light on the relationship between the Indosinian tectonic and magmatic activity in the region. Three precise zircon U–Pb ages yielded a mean of 218 ± 0.8 Ma, which is taken as the age of crystallization. The pluton consists of both granodiorite (64.59–68.01 % SiO_2 and 3.25–4.22 % K_2O) and granite (70.49–71.80 % SiO_2 and 4.07–4.70 % K_2O). The granodiorites are characterized by relatively high Mg# (54–57), low contents of Na_2O (3.2–4.3 wt%), low abundances of incompatible elements (LILE, Nb and P), high initial $^{87}Sr/^{86}Sr$ (0.7175–0.7184) and negative $\varepsilon_{Nd}(t)$ (−9.98 to −9.72). REE patterns show moderate fractionation ($(La/Yb)_{cn}$ = 8.07–18.80) with negative Eu anomalies (Eu/Eu* = 0.62–0.86). Compared with the granodiorite, the granite has a wider range of Mg# (49–59), lower contents of Na_2O (2.8–4.2 wt%), higher initial $^{87}Sr/^{86}Sr$ (0.7232–0.7243) and more negative $\varepsilon_{Nd}(t)$ (−12.07 to −11.24) values. REE patterns are relatively flat ($(La/Yb)_{cn}$ = 14.73–29.37) with smaller negative Eu anomalies (Eu/Eu* = 0.48–0.63). The granodiorite has lower K_2O/Na_2O and $Al_2O_3/(MgO + FeO_{Tot})$ values than the granite. Based on major and trace element geochemistry and Sr–Nd isotopes, we interpret the Longtan granodioritic magma to have been derived by partial melting of interlayered Proterozoic metabasaltic to metatonalitic source rocks, whereas the granite was probably derived from a mixture of Proterozoic metagraywackes and metaigneous rocks. Field, petrographic and geochemical evidence indicate that partial melting and fractional crystallization were the dominant mechanism in the evolution of the pluton. The Longtan granodiorites and granites are petrologically and geochemically similar to typical Indosinian varieties and are considered to have been produced in a similar manner. The Indosinian granitoids in the region show a magmatic peak age of ~238 Ma from the Yunkai-Nanling belt in the southeast and a magmatic peak age of ~218 Ma of the Xuefengshan belt to the northwest. These early and late magmatic episodes of the Indosinian granitoids also display slight variations of regular compositions, $\varepsilon_{Nd}(t)$ values and T_{DM} ages. Thus, we propose a syncollisional extension model that Indosinian granitoids were generated by decompressional partial melting of crustal materials triggered by two extensions during collision of the Indochina and South

Electronic supplementary material The online version of this article (doi:10.1007/s00531-013-0996-z) contains supplementary material, which is available to authorized users.

L. Qiu · D.-P. Yan (✉) · S.-L. Tang
State Key Laboratory of Geological Processes and Mineral Resources, School of Earth Sciences and Resources, China University of Geosciences, Beijing 100083, China
e-mail: yandp@cugb.edu.cn

L. Qiu
Department of Geoscience, University of Nevada, Las Vegas, Las Vegas, NV, USA

M.-F. Zhou · S.-L. Tang
Department of Earth Sciences, The University of Hong Kong, Pokfulam Road, Hong Kong, China

N. T. Arndt
ISTerre, Université de Grenoble, Grenoble, France

L. Qi
State Key Laboratory of Ore Deposit Geochemistry, Institute of Geochemistry, Chinese Academy of Sciences, Guiyang 550002, China

Published online: 21 January 2014

China blocks. The Longtan pluton in the northwesternmost part of the orogenic belt marks the termination of the Indosinian magmatism and orogenesis.

Keywords South China · Indosinian orogeny · High-K granodiorite and granite · Granitoid genesis · Partial melting · Fractional crystallization

Introduction

Granitoid plutons derived from crustal melting occur in a wide variety of tectonic settings, e.g., subduction zones, collision zones, rift zones and intraplate environments (Petford et al. 2000; Annen et al. 2006; Brown 2007; Xiao et al. 2009; Conrad et al. 2011; Le Pape et al. 2012). Seismic, magnetotelluric and gravity data of many orogens, including the central Andes and Himalayas, have identified the presence of partial melt within thickened continental crust (Schilling et al. 1997; Schmitz et al. 1997; Kalsbeek et al. 2001; Vanderhaeghe and Teyssier 2001; Wang et al. 2013). Additionally, there is abundant evidence for the presence of partial melt in deeply exhumed ancient orogens (e.g., Vanderhaeghe and Teyssier 2001). The combined processes of crustal melting, ascent and emplacement of magma are considered significant material and heat transfer processes from deep to shallow crust (England and Thompson 1986; Simpson et al. 2000). Thus, the magma source and magma-forming process of crustal melting are key to understanding the evolution of continental crust which consists mainly of granitoids (Altherr et al. 2000; Annen et al. 2006; Brown 2007).

The tectonic configuration of Southeast Asia is the consequence of amalgamation of microcontinents from the Early Triassic to the present. The Indosinian orogeny, which was defined originally by Triassic angular unconformities in Vietnam and South China (Deprat 1914; Fromaget 1932, 1941), is thought to have been caused by continental collision between the Indochina and South China blocks (SCB) during closure of the eastern Paleo-Tethys Ocean (Cho et al. 2008). Previous studies of the Late Permian to Triassic granitoids in the SCB (e.g., Huang et al. 1987; Chen and Jahn 1998; Shen et al. 1998; Deng et al. 2004; Chen et al. 2007, 2011, 2013; Zhou et al. 2008; Mao et al. 2011; Yang et al. 2012; Charvet 2013; Wang et al. 2001, 2002, 2007, 2013) have shown that Indosinian granitoids in the Yunkai-Nanling belt in the southeast are strongly peraluminous, whereas those in the Xuefengshan belt in the interior of the SCB are weakly to moderate peraluminous.

However, the timing of the Indosinian orogeny, the origin of the granitoids and the regional tectonic framework are still not clear (Carter et al. 2001; Lepvrier et al. 2004). Numerous tectonomagmatic models have been proposed to explain the patterns of deformation and magmatism of this orogen. For example, Li and Li (2007) proposed that flat-slab subduction of the Pacific plate was responsible for development of the broad, Laramide-style magmatic province in the SCB during the Triassic to Early Jurassic. Lepvrier et al. (2004, 2008), Zhou et al. (2006) and Shu et al. (2008) proposed that Indosinian magmatism was caused by northward subduction and collision of the Indochina block with the SCB in response to closure of the Paleo-Tethys Ocean. Wang et al. (2007) suggested that the Indosinian granitoids might have resulted from intracontinental collision between the Yangtze and Cathaysian blocks. Additionally, Chu et al. (2012a, b) suggested that the Early Mesozoic granites may be late-orogenic products of the intracontinental Xuefengshan orogen produced by subduction of the Paleo-Pacific ocean plate. However, none of these models adequately explain the wide distribution of the Indosinian granitoids, particularly variations in age over a distance of ca. 1,200 km. Most workers in the region agree that the granitoids were derived from Precambrian crustal basement (e.g., Ge 2003; Deng et al. 2004; Wang et al. 2007), and Wang et al. (2002, 2007, 2013) specifically proposed that the magmatic activity was related isostatic adjustment, in situ radiogenic heating, and magmatic underplating of a thickened crust.

Although many studies have focused on the Indosinian granitoids in the SCB, little attention has been paid to the crustal melting processes or to defining the northern margin of the orogen (Faure et al. 1996; Xiao and He 2005; Lin et al. 2008). Additionally, there are no systematic geochemical studies of the Indosinian granitoids can be used to understand the time–space pattern and termination of the Indosinian tectonomagmatism (Wang et al. 2013). The Longtan pluton, one of the youngest Indosinian plutons in the region, is located in the northwesternmost part of the orogenic belt and contains rocks compositionally similar to Indosinian granitoids elsewhere in the SCB (Fig. 1; BGMRHN 1988; Chen and Jahn 1998; Wang et al. 2002, 2005a; Mao et al. 2011). In this paper, we present new precise SIMS zircon U–Pb ages, major and trace element data, and Sr–Nd isotopes values for the Longtan granodiorites and granites. We then use these new data with previously published information on Indosinian granitoids of the entire SCB to constrain the origin, time–space patterns and termination of Indosinian magmatism.

Geologic background

Tectonic framework and sedimentary sequence

The SCB is composed of the Yangtze block to the northwest and Cathaysian block to the southeast (Fig. 1a; Ren

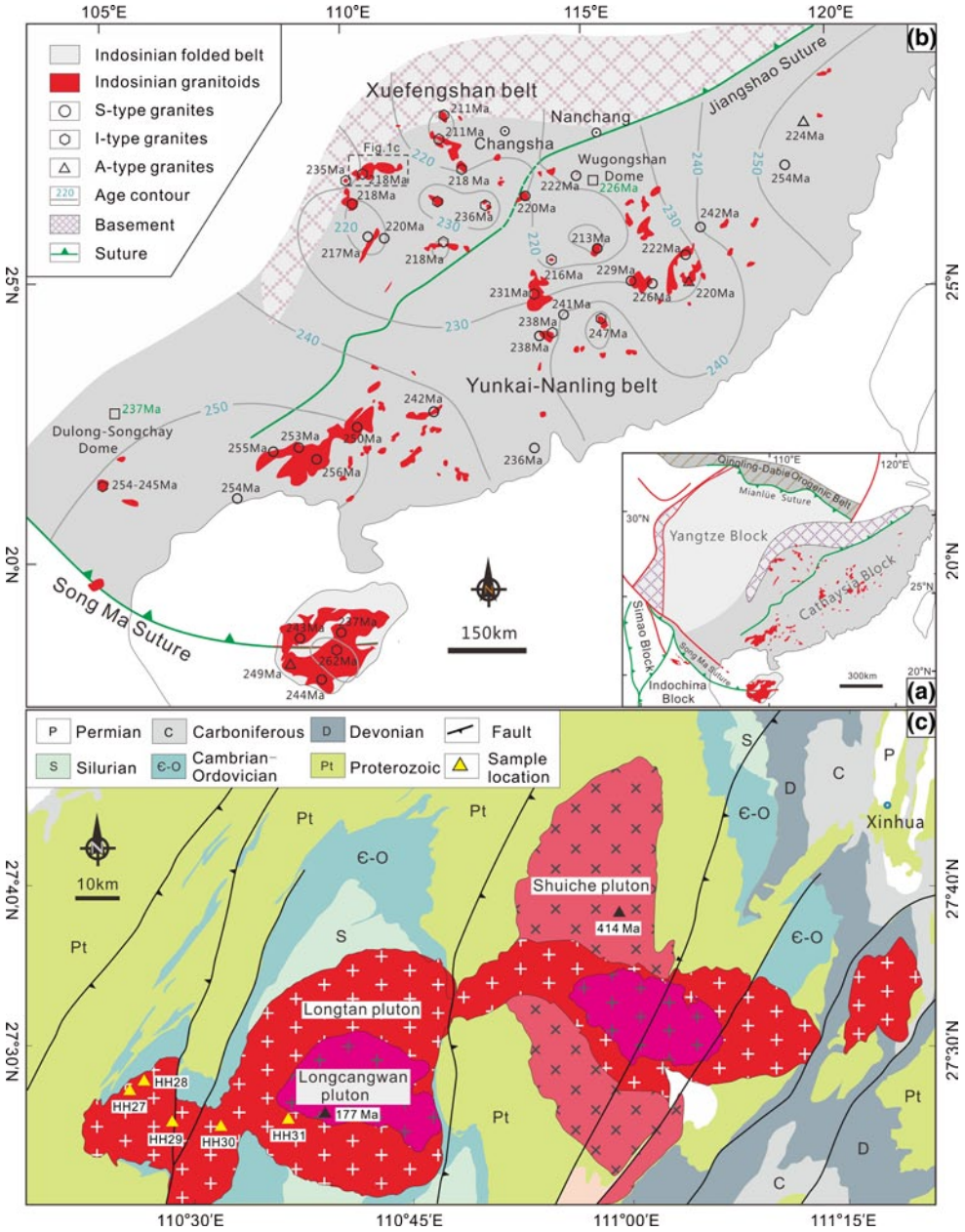

Fig. 1 **a** Sketch map of major microcontinents and suture zones of the South China and Indochina blocks in the Southeast Asia (Carter et al. 2001; Yan et al. 2003, 2006; Metcalfe 2006; Zhou et al. 2006, 2008; Lin et al. 2008). **b** Exposed 210–260 Ma granitoids in the SCB. Representative ages (Ma) of Indosinian plutons and data of age contour are from Li and Li (2007), Wang et al. (2005a, b), Zhou et al. (2006) and references shown in Supplementary Table 5. **c** Geological map of the Longtan pluton and adjacent regions showing petrology and structure in the plutons (modified after BGMRHN 1988, 1995a, b; Chen et al. 2007). The symbols of yellow triangles refer to sampling locations

1996; Yan et al. 2003). The two blocks have a folded and metamorphosed basement composed of the Mesoproterozoic to Neoproterozoic Sibao and Banxi groups and their equivalents (Zhao et al. 2011). The Sibao group is dominated by epimetamorphic sandy-argillaceous detrital rocks with flysch and volcanic intercalations (BGMRGX 1985; Zhao et al. 2013a, b). The Banxi group consists of a graywacke-schist succession, tillite, limestone and volcanic rocks (BGMRHN 1988; Zhou et al. 2002; Wang and Li 2003). The sedimentary cover is composed mainly of folded Paleozoic and Lower Triassic strata of shallow marine origin, and Middle Triassic to Cretaceous clastic rocks (Metcalfe 2011; Wang et al. 2013). The Indochina block is an amalgamation of several terranes that are separated by suture zones (Fig. 1a; Fan 2000; Metcalfe 2002, 2011; Yan et al. 2006). The major amalgamation, related to the Indosinian orogeny, was produced by collision between the Indochina and adjacent blocks (Deprat 1914; Fromaget 1927, 1941; Lacassin et al. 1998; Lepvrier et al. 2008). The main phase of this collision is constrained at 258–243 Ma by U–Pb zircon ages of metamorphic basement in Vietnam (Carter et al. 2001).

Numerous suture zones, which were produced by closure of the Paleo-Tethys Ocean, subdivide and separate the SCB from adjacent blocks (Fig. 1a). The Neoproterozoic to Early Paleozoic Jiangshao suture zone separates

the Yangtze block from the Cathaysian block within the SCB (Ren 1996; Charvet et al. 1996; Yan et al. 2006; Wan 2011). The Indochina block is separated from the SCB by the Paleozoic to Triassic Song Ma suture zone (Hutchison 1975; Carter et al. 2001; Metcalfe 2006; Shu et al. 2008; Faure et al. 2013), which contains strongly sheared mafic and ultramafic rocks regarded as elements of a disrupted ophiolite (Fromaget 1941; Lepvrier et al. 2004; Trung et al. 2006). The Triassic Mianlüe suture separates the Qinling-Dabie orogenic belt from the SCB (Ratschbacher et al. 2003; Lai et al. 2004; Zhang et al. 2004a, b).

Indosinian magmatism

Indosinian granitoids occur as voluminous, peraluminous batholiths and widely dispersed small intrusions within the SCB (Fig. 1b; BGMRJX 1984; BGMRHN 1988; Mao et al. 2011). They consist of 60 % (outcrop area) strongly peraluminous (A/CNK > 1.1) S-type granitoids (Deng et al. 2004; Sun et al. 2005), 30 % weakly peraluminous (A/CNK = 1.0–1.1) and 10 % calc-alkaline I-type granitoids. The strongly peraluminous granitoids contain minor mafic enclaves (Wang et al. 2007; Zhao et al. 2010), but the weakly peraluminous granitoids contain abundant angular to rounded mafic enclaves and sparse hornblende. The only known Indosinian mafic rocks are the enclaves in the granitoids (Wang et al. 2007). The Indosinian granitoids have ages ranging from ca. 260 to 210 Ma based on various techniques (e.g., Chen et al. 2007, 2011; Chu et al. 2012a, b; Wang et al. 2007, 2013).

The Longtan pluton

The Longtan pluton, which is located in the central part of the Xuefengshan belt in the interior of the SCB, is one of the northwesternmost outcrop plutons (Fig. 1c). This EW-striking, ellipsoidal granitoid was emplaced into the Silurian monzogranitic Shuiche pluton (414 ± 4 Ma; Chu et al. 2012a, b) and was later intruded by the Jurassic monzogranitic Longcangwan pluton (177 ± 1.7 Ma; Chen et al. 2007).

The pluton is composed of fine- to medium-grained biotite granodiorite and medium- to coarse-grained granite (Fig. 2a, b, e, f). Lath-shaped feldspar phenocrysts with a grain size of 0.8–3.5 cm are common in the granite. Ellipsoidal mafic microgranular enclaves (MMEs), 10–30 cm in diameter (Fig. 2c), and fine-grained granitic enclaves with maximum diameter of 90 cm are also present. The MMEs and elongated xenoliths with a gneissic texture are particularly common in the marginal zone (Fig. 2d; Zhuang et al. 1988; Chen et al. 1998, 2007; Wang et al. 2005a).

Previous workers have reported a wide range of ages for the Longtan pluton, from a low of 205 ± 2.2 Ma (LA-ICPMS; Luo et al. 2010) to a high of 243 ± 3 Ma (SHRIMP zircon U–Pb; Wang et al. 2007). Some of these ages are difficult to evaluate, because of poor precision of the dating method or a lack of detail about the morphology and texture of the zircon grains (Chen et al. 1986; BGMRHN 1995a, b).

Sampling and analytical methods

Samples were collected from the margin to the center in the western part of the Longtan pluton (Fig. 1c). Three samples HH27-5, HH29-5 and HH31-8 were selected for zircon U–Pb analyses. Thirty-four fresh whole-rock samples were collected for major and trace element analyses and nine samples were selected for Sr–Nd isotopic analyses.

SIMS Zircon U–Pb dating

Zircons were separated from fresh samples by using standard heavy liquid and magnetic techniques. Zircon grains, together with the zircon standards DC-13, Qing Hu and Plesovice (Mattinson 2005; Li et al. 2009), were mounted in epoxy, polished and vacuum coated with high-purity gold. The shapes and internal textures of all the zircons were documented with transmitted and reflected light microscopy, as well as cathodoluminescence (CL) images to reveal their internal structures. CL images of zircons were taken using a JXA-8100 Cameca electron probe at a voltage of 15 kV and current of 10 nA at the Institute of Geology and Geophysics, Chinese Academy of Sciences. Measurements of U, Th and Pb isotopes were conducted using a newly installed Cameca IMS 1280 large-radius SIMS at the same institute. Analytical procedures are those described by Li et al. (2009, 2010). Data were processed using the GLITTER, ISOPLOT and CGDK programs (Ludwig 2003; Qiu et al. 2013).

Major and trace element analysis

Major oxides were analyzed with a PANalytical Axios-advance (Axios PW4400) X-ray fluorescence spectrometer (XRF) at the State Key Laboratory of Ore Deposit Geochemistry, Institute of Geochemistry, Chinese Academy of Sciences (IGCAS). Loss on ignition (LOI) was obtained using 1 g of powder, which was heated to 1,100 °C for 1 h. Major oxides were measured on fused glass with a precision better than 2 %.

Trace elements were analyzed using a Perkin-Elmer Sciex ELAN 6000 ICP-MS at the IGCAS. The powdered samples (50 mg) were dissolved in a mixture of HF + HNO_3 in

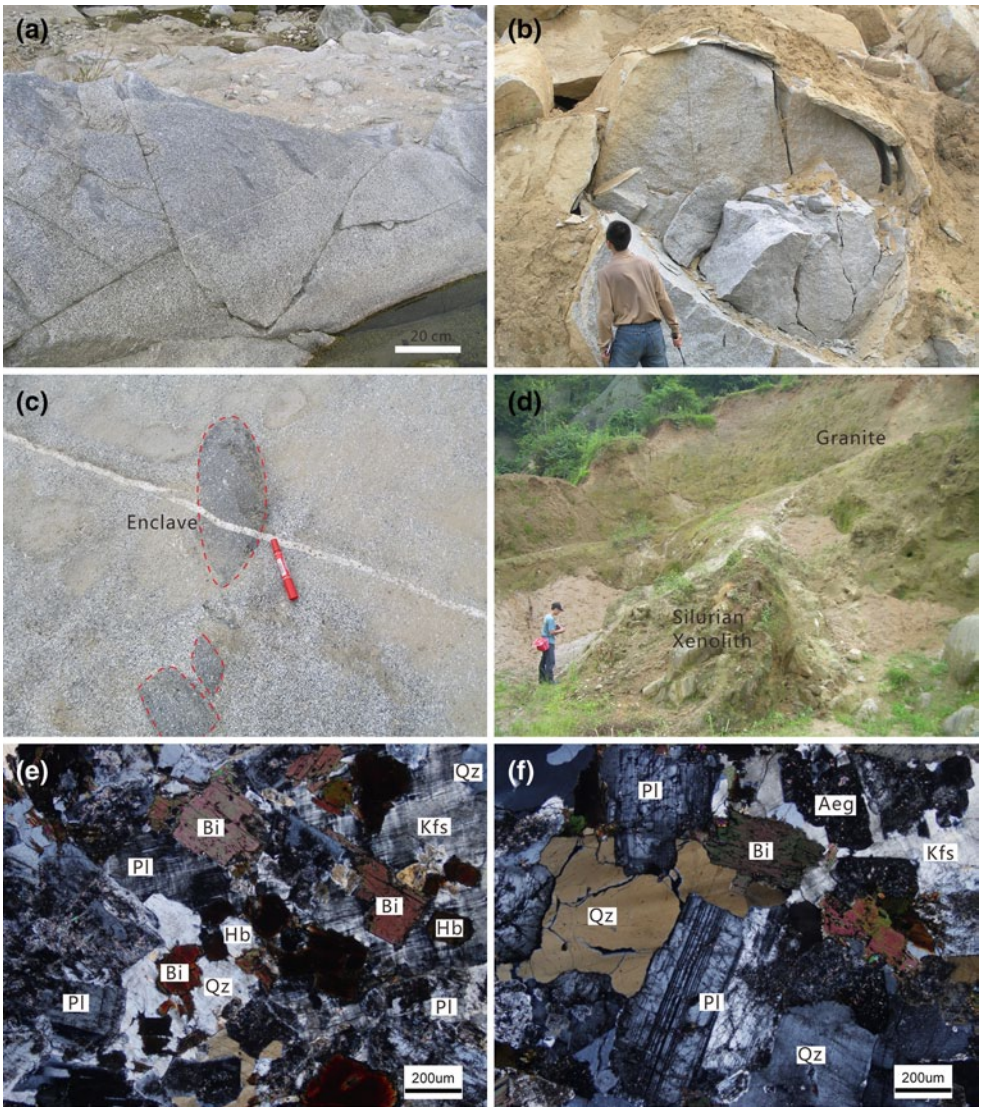

Fig. 2 Field photographs and microphotographs of the granitoids from the Longtan pluton in the SCB. **a** Fine-grained granodiorite; **b** coarse-grained granite; **c** mafic microgranular enclave; **d** Silurian xenoliths; **e** microphotograph of granodiorite; **f** microphotograph of granite. Length of the marking pen is 14 cm

high-pressure Teflon bombs for 48 h at ca. 190 °C (Qi et al. 2000). Rhodium was used as an internal standard to monitor signal drift during counting. Repeated analyses of international standard GBPG-1 were used for analytical quality control. Analyses of international standards OU-6 and GBPG-1 are in agreement with recommended values. The analytical precision was generally better than 5 % for all elements.

Whole-rock Sr–Nd isotopic analysis

Sr and Nd isotopic ratios were analyzed at the IGCAS. $^{87}Rb/^{86}Sr$ and $^{147}Sm/^{144}Nd$ ratios were calculated using the Sr and Nd abundances measured by ICP-MS. Several analyses on the NBS-987 Sr standard yielded $^{87}Sr/^{86}Sr = 0.710254 \pm 5$. Mean $^{143}Nd/^{144}Nd$ ratios for the Jndi-1 Nd standard were 0.512078 ± 7. $^{143}Nd/^{144}Nd$ ratios were normalized to the value of $^{146}Nd/^{144}Nd = 0.7219$. Fractionation effects during the Sr isotopic composition runs were eliminated by normalizing to an $^{86}Sr/^{88}Sr$ value of 0.1194. Detailed procedures are available in Xu et al. (2007).

Analytical results

SIMS zircon U–Pb ages

Zircons from sample HH27-5 (granodiorite) have pyramidal and prismatic crystal forms, inherited cores and

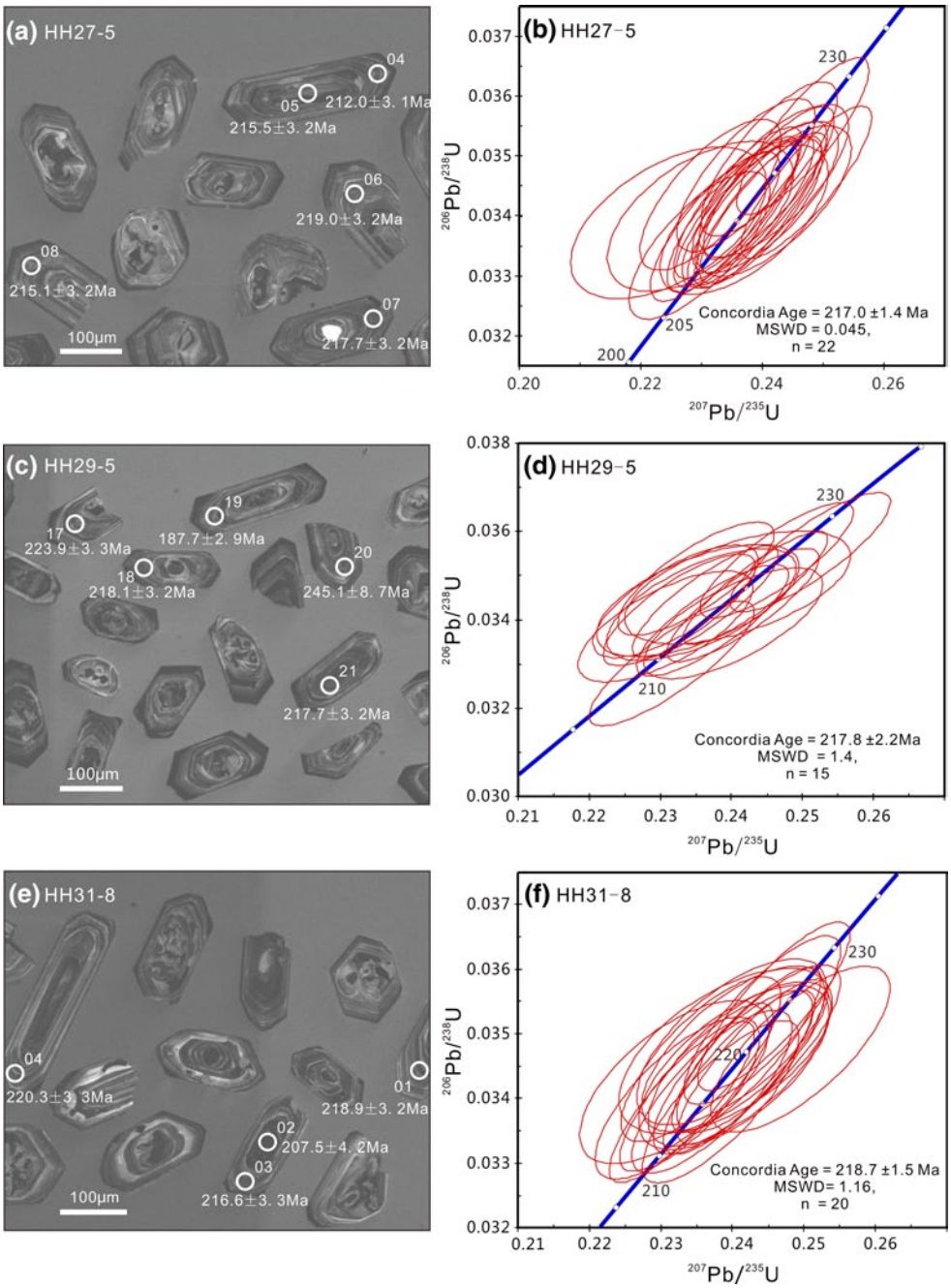

Fig. 3 Representative cathodoluminescence images of zircon grains and corresponding SIMS zircon U–Pb concordia diagram of the granitoid samples from the Longtan pluton

magmatic oscillatory in CL images (Fig. 3a). They are 70–290 μm long with length/width ratios ranging from 1:1 to 3:1. All of zircons with Th/U ratios between 0.39 and 2.5 show igneous or inherited cores. Three of 25 analyses have significant percentages of common ^{206}Pb and were discarded. The remaining 22 analyses give a concordia U–Pb age of 217.0 ± 1.4 Ma (2σ error) with a small MSWD of 0.045 (Fig. 3b; Supplementary Table 1).

Zircons from sample HH29-5 (granite) have oscillatory zonal textures with Th/U ratios of ca. 0.40–1.35, indicating an igneous origin (Zhou et al. 2002). They are 40–280 μm long with length/width ratios ranging from 1:1 to 3:1 in CL images (Fig. 3c). Ten analyses that have $f_{206}(\%)$ values significantly higher than the detector background and 1 analysis with a Th/U ratio less than 0.1 are excluded in the age calculation (Supplementary Table 1). Treated as a single group, the remaining 15 analyses yield a concordia U–Pb age of 217.8 ± 2.2 Ma (MSWD = 1.4; Fig. 3d).

Zircons from sample HH31-8 (granodiorite) exhibit euhedral, pyramidal and prismatic shapes and magmatic oscillatory zoning, with a minority of grains exhibiting inherited cores and magmatic rims. Lengths range from 40

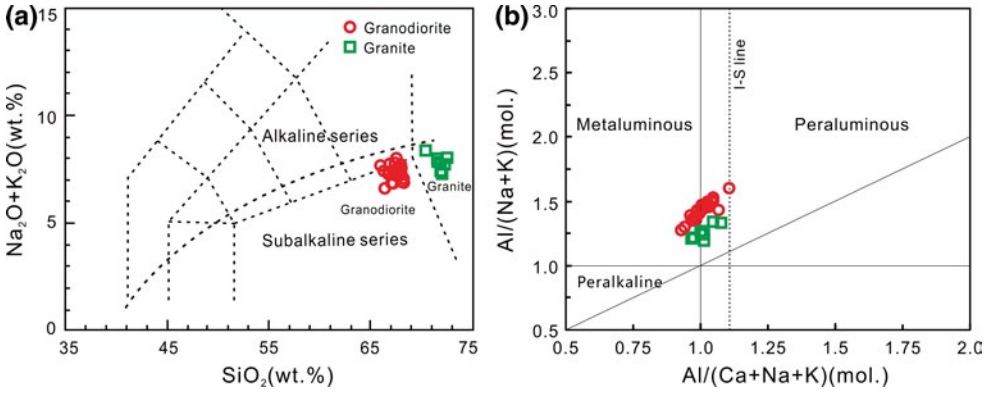

Fig. 4 Classification of the granitoids: **a** TAS diagram. All of the major element data have been recalculated to 100 % on a LOI-free basis (Middlemost 1994; Le Maitre 2002); **b** molar $Al_2O_3/(Na_2O + K_2O)$ versus molar $Al_2O_3/(CaO + Na_2O + K_2O)$ plot (Chappell and White 1992; Chappell 1999)

to 320 μm yielding length/width ratios of 1:1–4:1 (Fig. 3e). Twenty-four analyses with Th/U ratios from 0.39 to 1.04 were obtained (Supplementary Table 1). Four analyses have f_{206}(%) values significantly higher than the detector background and are excluded in the age calculation. The remaining 20 analyses yield a concordia U–Pb age of 218.7 ± 1.5 Ma (MSWD = 1.16; Fig. 3f).

The three samples have identical ages within the uncertainty of the analyses, so we use all 57 analyses from the three samples to obtain a weighted mean $^{206}Pb/^{238}U$ age of 218 ± 0.8 Ma (MSWD = 3.2; 95 % confidence), precisely constraining the age of emplacement of the Longtan pluton.

Major and trace elements

Thirty-four samples from the Longtan pluton exhibit a narrow range of chemical compositions (Supplementary Table 2; Fig. 4). All samples belong to the granodiorite and granite series on a total alkali-silica diagram (Fig. 4a; Middlemost 1994; Le Maitre 2002) and show a high-potassic calc-alkaline affinity on the SiO_2 versus K_2O diagram (Fig. 5a; Morrison 1980; Roberts and Clemens 1993). The two groups are easily distinguished; granodiorites have 64.6–67.5 % SiO_2 and granites have 70.5–71.8 % SiO_2 (Fig. 4a). Both groups straddle the boundary between metaluminous and peraluminous fields, with A/CNK ratios from 0.93 to 1.10 (Chappell 1999), and they plot in the field of I-type granitoids (Chappell and White 1992; Figs. 4b, 5e). There are significant negative correlations between SiO_2 and MgO, CaO, Fe_2O_3, P_2O_5, TiO_2 and Zr, and positive correlations between SiO_2 and K_2O and Rb on the Harker diagrams (Fig. 5).

Both granodiorites and granites have similar chondrite-normalized REE patterns with moderate to strong LREE enrichment ($(La/Yb)_{cn}$ = 8.07–29.37), prominent negative Eu anomalies (Eu_N/Eu^* = 0.48–0.86) and moderate HREE fractionation ($(Gd/Yb)_{cn}$ = 0.88–1.32) (Supplementary Table 2; Fig. 6a). On the mantle-normalized trace element diagram (Fig. 6b), both granodiorites and granites display strong enrichment of Pb and depletion of Ba, Nb, Sr, P and Ti. The granodiorites show a moderate fractionated REE pattern with LREE/HREE ratios of 7.22–13.72, $(La/Yb)_{cn}$ = 8.07–18.80 and Eu/Eu* ratios (0.62–0.86), but the granites display strongly fractionated REE patterns with lower LREE/HREE ratios (11.35–16.69) and more significant HREE fractionation $(La/Yb)_{cn}$ = 14.73–29.37 and Eu/Eu* ratios (0.48–0.63) (Supplementary Table 2; Fig. 6a). The granodiorites show shallower Ti troughs (2,641–3,485 ppm) than the granites (1,323–2,060 ppm).

Whole-rock Sr–Nd isotopes

The granodiorites exhibit lower initial $^{87}Sr/^{86}Sr$ ratios (0.7175–0.7184) but higher $\varepsilon_{Nd}(t)$ value (−9.98 to −9.72) (Supplementary Table 3; Fig. 9a), and model ages (T_{DM}) varying from 1.65 to 1.76 Ga (except for sample HH31-17, T_{DM} = 1.51). The initial $^{87}Sr/^{86}Sr$ ratios and $\varepsilon_{Nd}(t)$ values of the granites are from 0.7232 to 0.7243 and from −12.07 to −11.24, respectively. Model ages (T_{DM}) of the granites are from 1.78 to 1.84 Ga.

Discussion

Petrogenesis: magma source, partial melting and fractional crystallization

High-K granodioritic to granitic magmas found in collisional settings are mainly generated by (1) melting of crustal rocks by decompression or thermal relaxation (e.g., Roberts and Clemens 1993; Thompson et al. 1995; Petford et al. 2000); or (2) ascending parent mantle melts contaminated by crustal material (e.g., Hildreth and Moorbath 1988; Altherr et al. 2000). The geochemical characteristics [high K_2O, FeO/MgO ratios (1.7–2.0), enrichment of Rb, Ba, Pb, LREE and initial $^{87}Sr/^{86}Sr$ ratios; negative Nb and $\varepsilon_{Nd}(t)$ values; low Zr values (<8.4 %) and 10,000 Ga/Al

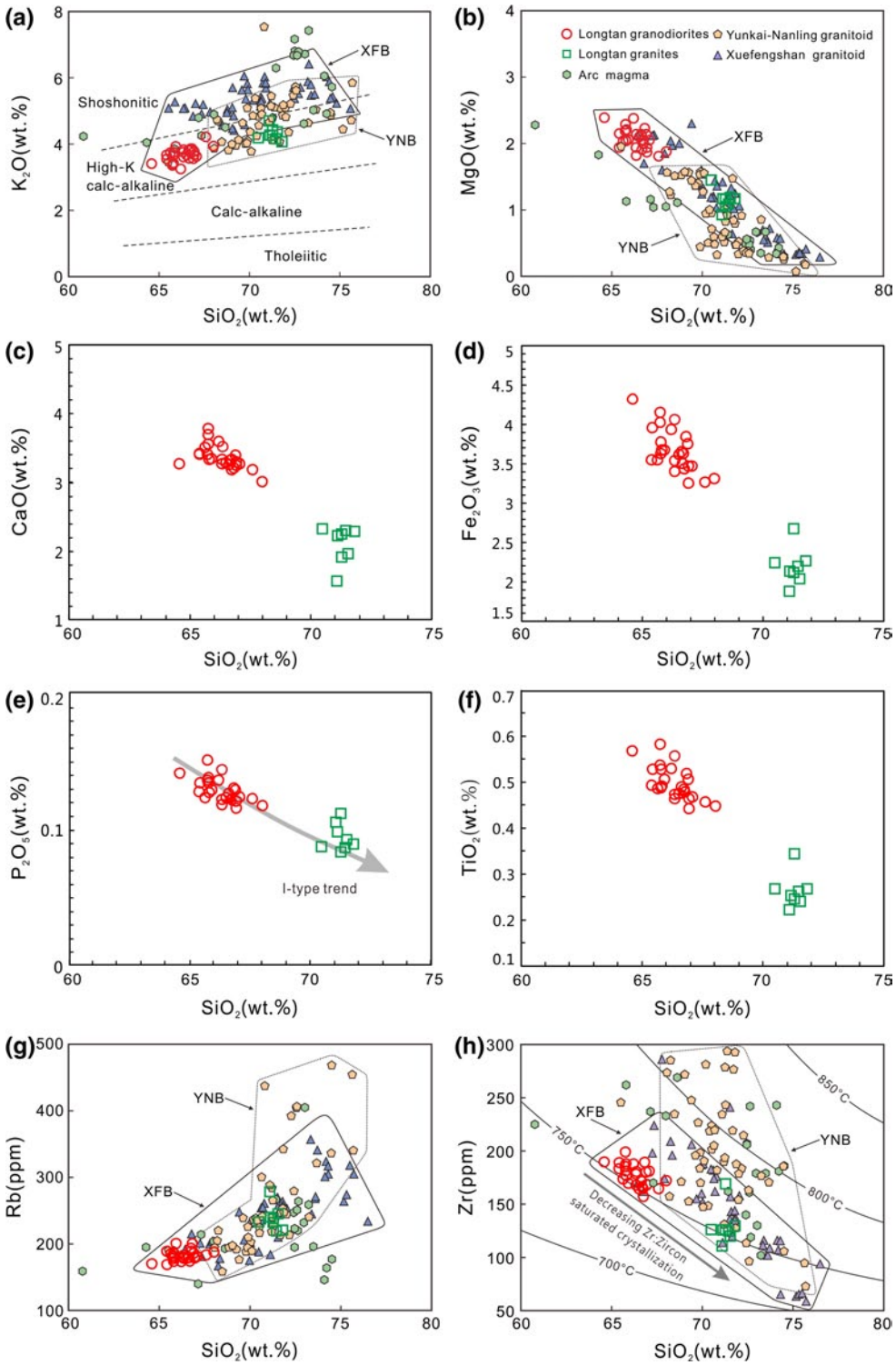

Fig. 5 Chemical variation diagrams of K_2O, MgO, CaO, Fe_2O_3, P_2O_5, TiO_2, Rb and Zr versus SiO_2 contents of the Longtan granitoids. The geochemical data of the granitoids in Yunkai-Nanling and Xuefengshan belts in the SCB are from Li et al. (2006), Sun et al. (2005), Xie et al. (2006), Chen et al. (2007), Qi et al. (2007), Wang et al. (2007), Yu et al. (2007), Charoy and Barbey (2008) and this study. The classification of the high-K, calc-alkaline series is from Roberts and Clemens (1993). The I-type trend is after Li et al. (2006). The generalized trajectory of the accumulative magmas (thin gray line) during in situ crystallization is from Kemp et al. (2005). *YNB* Yunkai-Nanling belt; *XFB* Xuefengshan belt

ratios (2.01–2.36)] of the Longtan granodiorites and granites all indicate crustal source (Collins et al. 1982; Chauvel et al. 1987; Whalen et al. 1987; Jung et al. 2000; Chen et al. 2007; Wang et al. 2007). The high-K, calc-alkaline, I-type affinity of the granodiorites and granites suggest a source composed of metasedimentary/metaigneous rocks (Roberts and Clemens 1993; Altherr et al. 2000). Furthermore, the similarity of REE patterns, $\varepsilon_{Nd}(t)$ values, model ages, strong enrichment of Pb and depletion of the HFSE between the Longtan granodiorites and granites and Proterozoic basement rocks indicate a genetic affinity (Figs. 6, 9; Li 1994; Chen and Jahn 1998; Shen et al. 1998; Wang

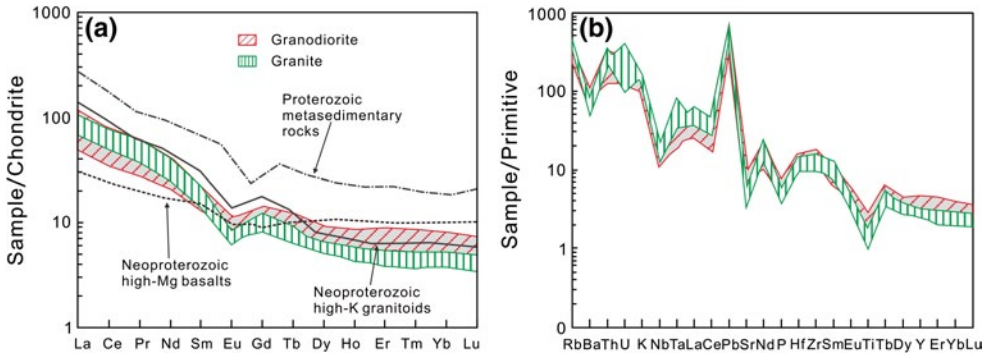

Fig. 6 **a** Chondrite-normalized REE patterns (normalizing values are from Sun and McDonough 1989) and **b** primitive mantle-normalized trace element spider diagram (normalizing values are from Taylor and McLennan 1985)

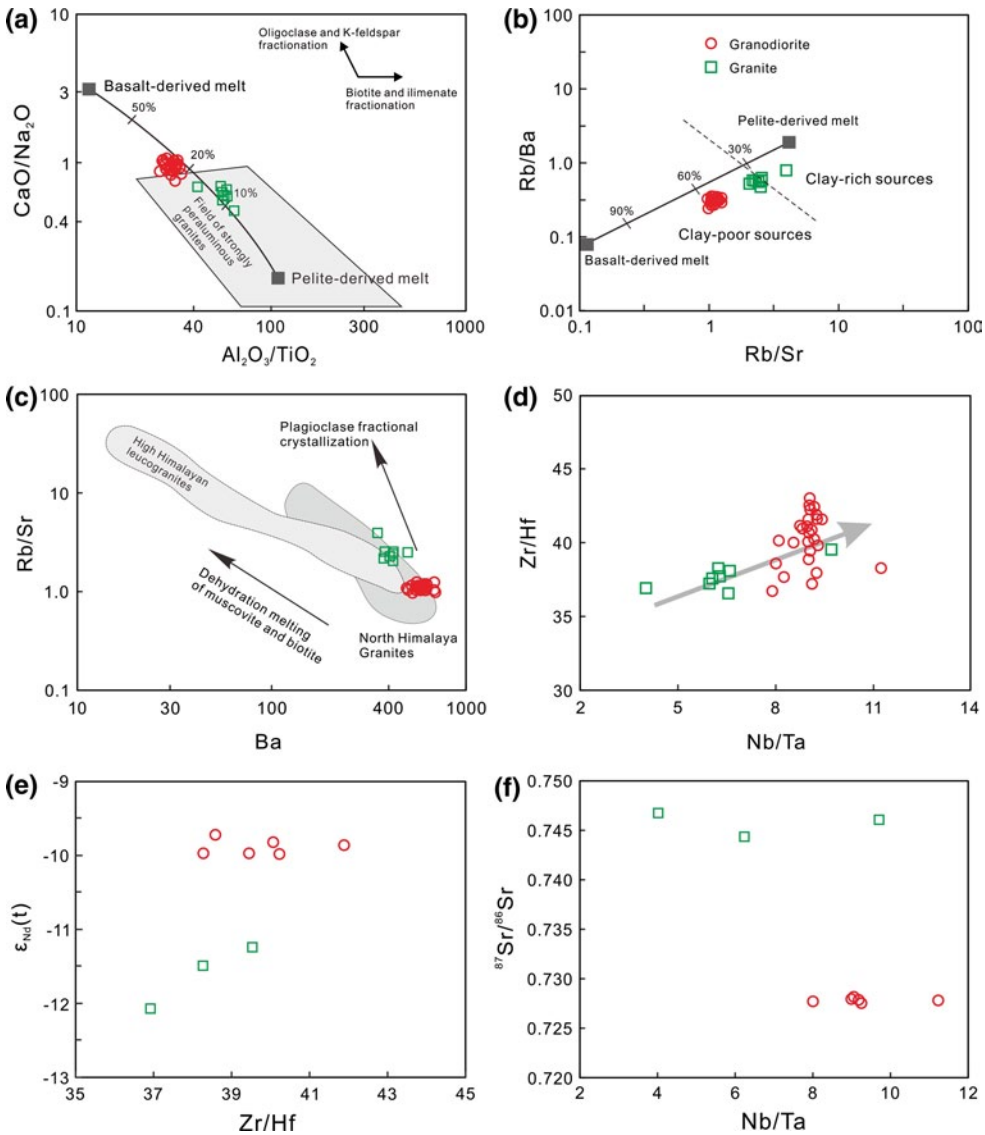

Fig. 7 **a** Al_2O_3/TiO_2 vs. CaO/Na_2O; **b** Rb/Sr versus Rb/Ba; **c** Ba versus Rb/Sr; **d** Nb/Ta versus Zr/Hf; **e** $\varepsilon_{Nd}(t)$ versus Zr/Hf; **f** Nb/Ta versus $^{87}Sr/^{86}Sr$. The mixing curve between the basalt- and pelite-derived melts is from Sylvester (1998). Peraluminous high Himalayan leucogranites and North Himalayan granites are from Inger and Harris (1993) and Zhang et al. (2004a, b)

et al. 2007; Wan et al. 2010; Zhao et al. 2013a, b). For example, on a t–$\varepsilon_{Nd}(t)$ diagram, all the granodiorites and granites plot in the field defined by the Proterozoic crust of the SCB and under the CHUR reference line (Fig. 9a; Shen et al. 1993).

The low ratios of CaO/Na_2O (granodiorite: 0.75–1.07; granite: 0.47–0.69), Rb/Ba (granodiorite: 0.24–0.35; granite: 0.47–0.79) and Rb/Sr (granodiorite: 0.97–1.25; granite: 2.05–3.94) indicate that the granodiorites and granites were derived from plagioclase-rich and clay-poor source

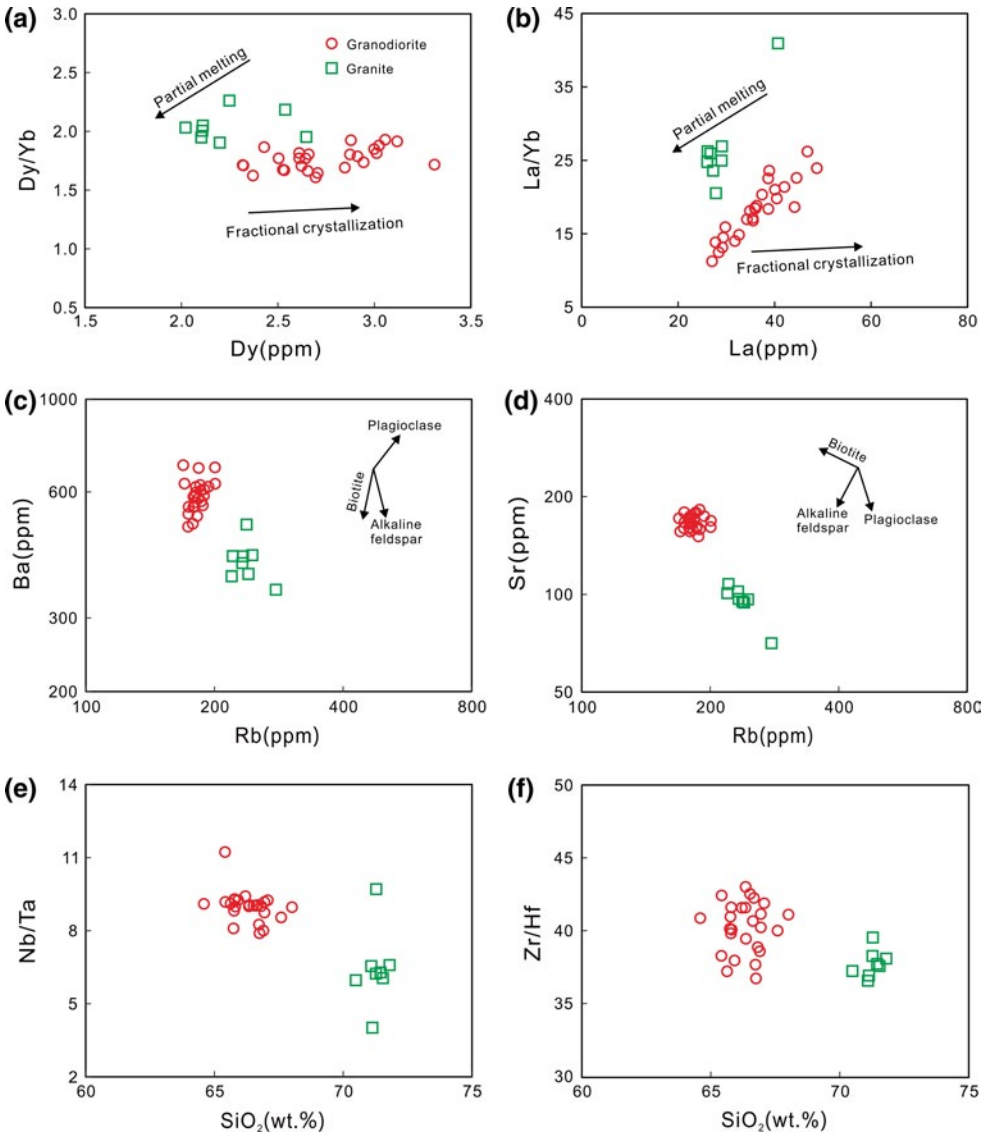

Fig. 8 Fractional crystallization vector diagrams. **a–d** Dy versus Dy/Yb, La versus La/Yb, Rb versus Ba and Sr diagrams for the Longtan granitoids. The trend of partial melting and fractional crystallization is from Wang et al. (2011). **e–f** SiO_2 versus Nb/Ta and Zr/Hf for the Longtan granitoids in the SCB. The trend of mineral crystallization is from Wang et al. (2007)

rocks (Fig. 7a–c; Chappell and White 1992; Sylvester 1998). The incompatible element diagrams [Rb/Sr vs. Rb/Ba, Ba (granodiorite: 579–696 ppm; granite: 351–501 ppm) vs. Rb/Sr and Nb/Ta vs. Zr/Hf (granodiorite: 7.89–11.23; granite: 4.02–9.71)] exhibit two discontinuous, distinct groups ruling out mixing of melts (Fig. 7b–d; Wang et al. 2007). On the plots of incompatible elements (Zr/Hf and Nb/Ta) versus isotopic compositions (Fig. 7e, f), both the granodiorites and granites show linear trends in these two diagrams but they clearly show that the groups are not related.

Compositional diversity of crustal magmas may correspond to variable melting conditions, such as pressure, temperature and H_2O content which control both the degree of partial melting (Patiño Douce and Beard 1995, 1996; Patiño Douce 1996; Jung et al. 2000), or unrelated magmas generated from different source rocks, such as metapelites, metagraywackes and metabasaltic to metatonalitic rocks (e.g., Gardien et al. 1995; Thompson 1996; Altherr et al. 2000; Wang et al. 2007). Based on molar oxide ratios, distinguishing the source of magmas with compositional variations generated by partial melting might available (Altherr et al. 2000). Partial melting produces granitoids with different K_2O/NaO ratios for different source rocks and with constant K_2O/NaO ratios and $K_2O > NaO$ for the same source rocks (Jung et al. 2000). Because most of the granodiorites and granites show different K_2O/NaO ratios, they were likely produced from different magma sources. The granodiorites have lower and $Al_2O_3/(MgO + FeO_{Tot})$ and K_2O/Na_2O ratios than the granites and their magmas were most likely derived from melting of metabasaltic to metatonalitic source rocks (Fig. 10c, d). The granites have chemical characteristics that are more compatible with a melting from mixing of

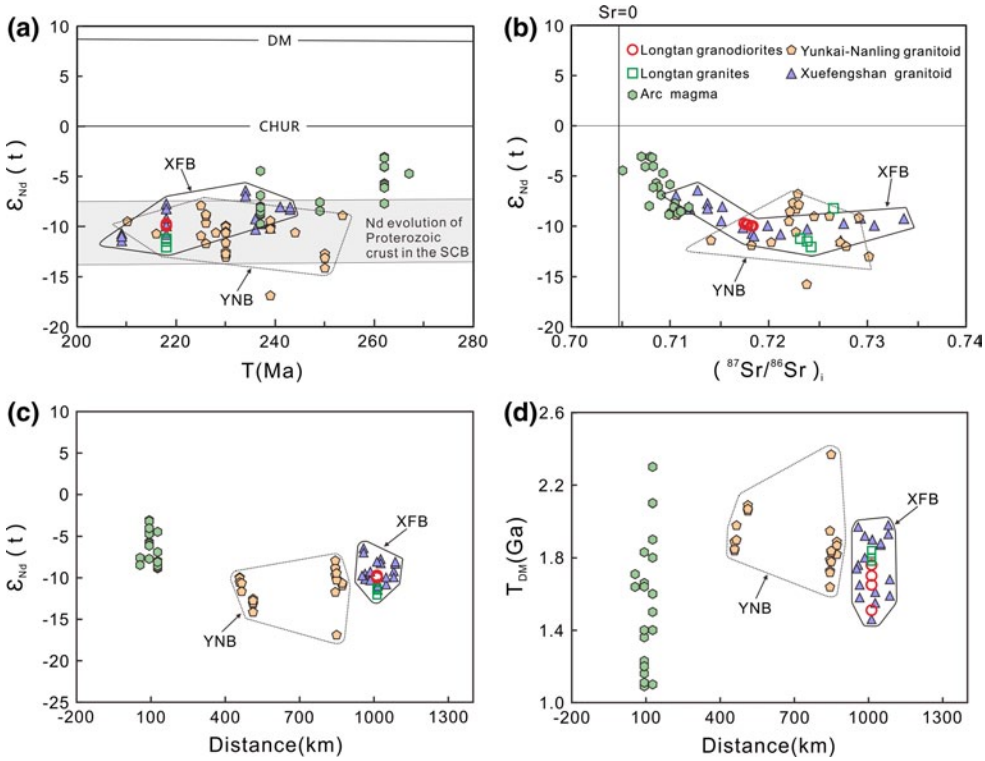

Fig. 9 Sr–Nd isotopes and T_{DM} age diagrams for granitoids from the Longtan pluton: **a**–**c** *t*, $(^{87}Sr/^{86}Sr)_i$ and distance versus $\varepsilon_{Nd}(t)$ diagram. The field for Nd evolution of the Proterozoic crust in the SCB is from Shen et al. (1993); **d** distance versus T_{DM} (Ga) diagram. The data are from Ge (2003), Li et al. (2006), Sun et al. (2005), Xie et al. (2006), Chen et al. (2007), Qi et al. (2007), Wang et al. (2007), Yu et al. (2007), Charoy and Barbey (2008) and this study. *YNB* Yunkai-Nanling belt, *XFB* Xuefengshan belt

metagraywackes and metabasaltic to metatonalitic source rocks. Due to their high CaO/(MgO + FeO_{Tot}) ratios (Fig. 10c), a significant contribution from metapelitic sources to the granodiorites and granites can be ruled out. Furthermore, higher CaO contents (>1.3 wt%), lower Rb/Ba (0.24–0.35), Rb/Sr ratios (0.97–1.25) and high Ba content (granodiorite: 579–696 ppm; granite: 351–501 ppm) of the granodiorite relative to the granite might be produced by H_2O-fluxing in a source of high feldspar and low mica (Inger and Harris 1993; Harris et al. 1995; Koester et al. 2002). For the granites, their high Rb/Sr ratios (2.05–3.94) and low Sr/Ba ratios (0.19–0.27) suggest granitic melts derived by muscovite-dehydration melting under water-undersaturated conditions (Rb/Sr: 2–6; Sr/Ba: 0.2–0.7; Harris and Inger 1992), which is similar in composition to Himalaya peraluminous granites and crustal-derived leucogranites (Fig. 7c; McDermott et al. 1996; Sylvester 1998). Compared with the granites, the granodiorites have abundances of Sr (granodiorite: 151–182 ppm; granite: 71–108 ppm), high Sr/Nd (granodiorite: 5.59–11.17; granite: 3.11–5.76) and Eu/Eu* ratios (granodiorite: 0.62–0.86; granite: 0.48–0.63) suggesting a smaller amount of plagioclase in their residues during partial melting. The granodiorites show more concentrated in values of Al_2O_3/(MgO + FeO_{Tot}), K_2O/Na_2O and CaO/(MgO + FeO_{Tot}) than the granites (Fig. 10c, d) and tend to have slightly higher Mg# at similar SiO_2 contents than the granites (Fig. 10a).

The granodiorites and granites define a negative Zr–SiO_2 trend (Fig. 5h), revealing the efficient saturated crystallization of zircon and a melt of this composition in equilibrium with zircon at ca. 750–800 °C (Fig. 5h; Kemp et al. 2005). This is also supported by experimental results (Vielzeuf and Schmidt 2001) suggesting that crustal metasedimentary/metaigneous rocks melts at low *P*–*T* conditions (<750 °C at moderate to high crustal pressures) (Brown 2013). Furthermore, under fluid-absent conditions (dehydration–melting), muscovite and biotite start to breakdown at ~700 and ~850 °C, respectively (Thompson 1996; Vielzeuf and Schmidt, 2001). Invariability and increasing of Nb/Ta and Zr/Hf ratios with increasing SiO_2 probably suggest the involvement and non-involvement of aqueous fluid phases for the granodiorites and granites, respectively (Fig. 8e, f).

Because of almost no compositional overlap between the granodiorites and granites, the genesis affinity of the two groups by fractional crystallization in homogeneous source is unlikely. As suggested by decreasing of MgO, CaO, Fe_2O_3, P_2O_5, TiO_2 and Zr with increasing SiO_2, fractional crystallization of plagioclase, biotite, apatite, K-feldspar and zircon are certainly important for the granodiorites (Fig. 5). Additionally, the granodiorites plot along the fractional crystallization trends on the Dy/Yb versus Dy diagram and along the partial melting trends in the La/Yb versus La diagrams (Fig. 8a, b; Wang et al. 2011), indicating that both partial melting and fractional

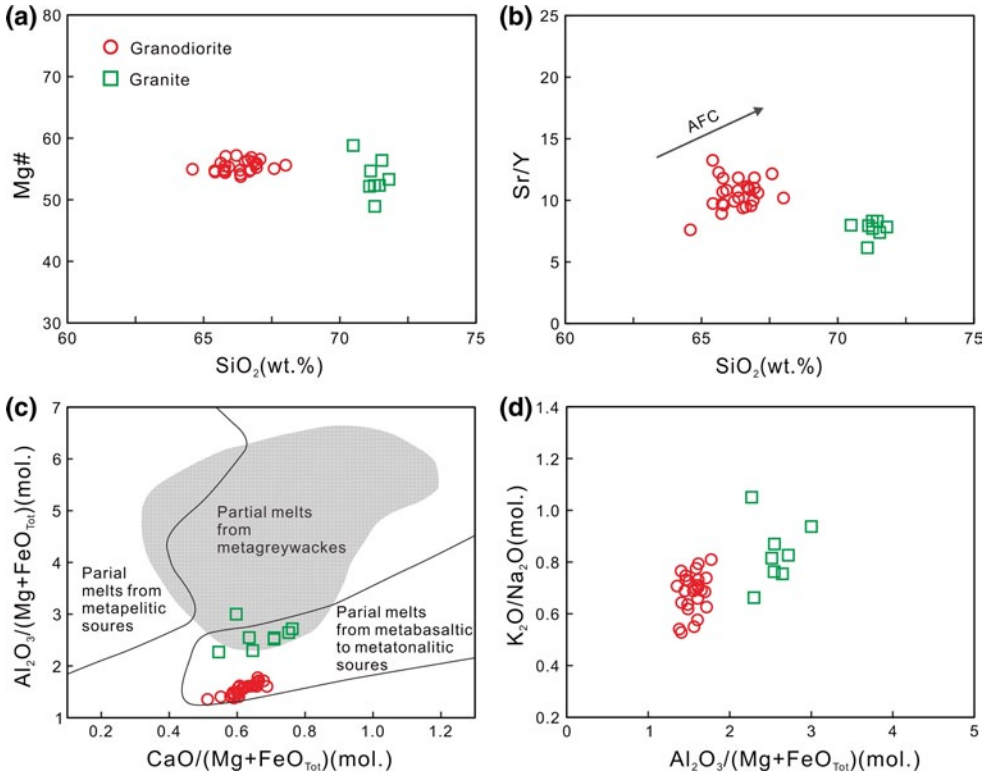

Fig. 10 Chemical compositions of I-type granitoids from the Longtan pluton in the SCB. **a** Mg# = molar 100*Mg/(MgO + 0.9*FeO_{Tot}) versus SiO_2 content; **b** Sr/Y versus SiO_2 content; **c** molar Al_2O_3/(MgO + FeO_{Tot}) versus molar CaO/(MgO + FeO_{Tot}). Outlined fields denote compositions of partial melts obtained in experimental studies by dehydration melting of various bulk compositions (Altherr et al. 2000); **d** molar K_2O/Na_2O versus molar Al_2O_3/(MgO + FeO_{Tot})

crystallization were involved in evolution of the Longtan granodiorites. It is recognized that the Rb–Ba and Rb–Sr variations (Fig. 8c, d) and strongly negative Ba, Nb, Sr, P and Ti anomalies (Fig. 6b) support fractionation of biotite for the granodiorites and possibly slight fractionation of plagioclase for granites. The concave-upward shape of REE patterns and negative Eu anomalies for the magmas indicate that plagioclase fractionated and amphibole-out boundary was not crossed during partial melting (Fig. 6a; Altherr et al. 2000). The lack of depletion in the HREE means that garnet was not a residual phase in the source material. The granites also show more fractionated REE patterns/higher LREE/HREE ratio and more significant Eu anomaly relative to the granodiorites (Fig. 6a). The presence of decreasing of Zr/Hf and Nb/Ta ratios for the granodiorites with increasing SiO_2 (Fig. 8e, f) and the distinct Sr–Nd isotopic compositions for the granodiorites and granites are not consistent with a closed-system fractional crystallization process (Dostal and Chatterjee 2000; Wang et al. 2007).

Consequently, the granodiorites might have been crustally derived by melting of interlayed Proterozoic metabasaltic to metatonalitic source rocks, whereas the granites were probably derived from muscovite-dehydration melting of Proterozoic metagraywackes and/or metaigneous source rocks. The melting conditions are probably under H_2O-fluxing and water-undersaturated for the granodiorites and granites at ca. 750–800 °C, respectively. Additionally, the magmas of granodiorites and granites yielded the same age, derived from different sources and were emplaced independently in the Longtan pluton without mixing of these two magmas. The granodiorites and granites were most likely formed from several magma pulses, or the granodiorites and granites represent separate intrusions with the undiscovered contact between them because of poor exposure.

Tectonic implications

The evaluation and synthesis of these new data in this study and previously published 130 age determinations of Indosinian granitoids in the orogenic belt show the Indosinian magma mainly emplaced in two stages, including early Indosinian with peak ages of ~238 Ma in the Yunkai-Nanling belt and late Indosinian with peak ages of ~218 Ma in the Xuefengshan belt, respectively (Fig. 11a, c; Supplementary Table 5 and criteria therein). The early Indosinian S-type granitoids in the Yunkai-Nanling belt show high A/CNK values (1.05–1.46), strongly negative Ba, Sr and Nb anomalies, a narrow range of REE patterns and relative high T_{DM} ages (2.09–1.82 Ga) (Supplementary Table 4; Fig. 9; Qi et al. 2007; Chen et al. 2011; Mao et al. 2011). These granitoids were derived by remelting of Proterozoic crustal materials under high crustal temperature (800–950 °C) and low pressure (4–6 kb) (Charoy and Barbey 2008). The late Indosinian granitoids in the Xuefengshan belt, typically the Longtan granodiorites and granites,

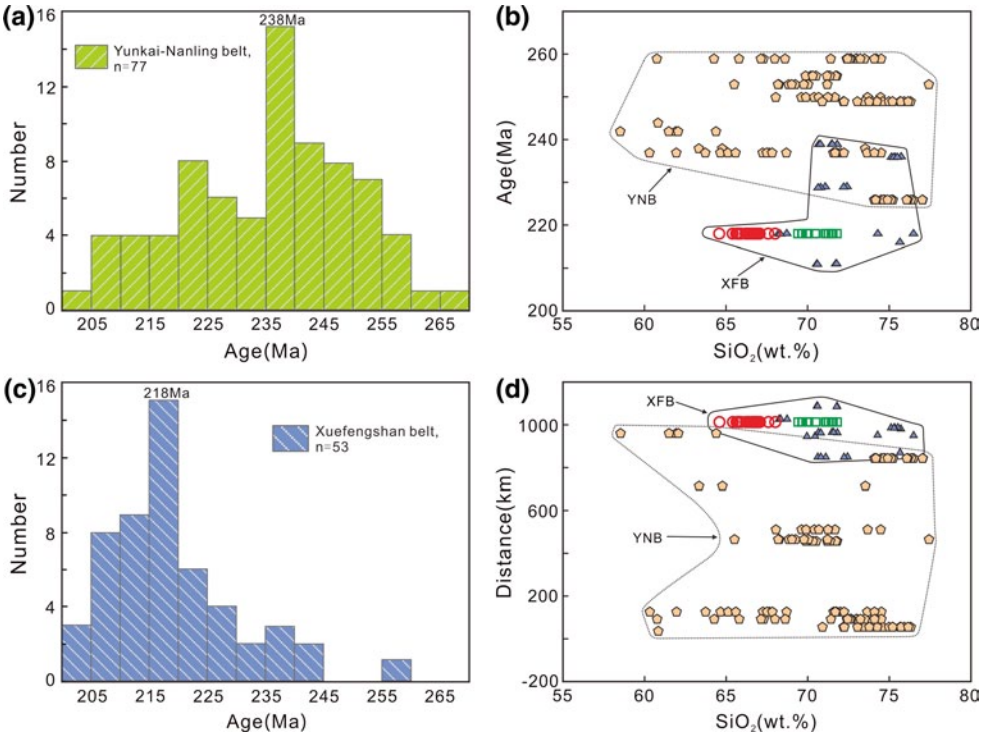

Fig. 11 **a**, **c** Frequency diagram of ages of Indosinian granitoids for the Yunkai-Nanling and Xuefengshan belts in the SCB, respectively; **b**–**d** SiO_2 contents versus age and distance for the granitoids from the Longtan pluton, Yunkai-Nanling and Xuefengshan belts in the SCB. The distance is from the southernmost Indosinian granitoid pluton to interior of the SCB. *YNB* Yunkai-Nanling belt; *XFB* Xuefengshan belt. *Symbols* are the same as those in Fig. 9

are peraluminous and also strongly negative Ba, Sr, Nb, P and Ti anomalies (Chen et al. 2007; Wang et al. 2007). The magmas were emplaced at relatively low temperature (734–827 °C) and have T_{DM} ages ranging from 1.46 to 1.98 Ga (Supplementary Table 4; Fig. 9d; Wang et al. 2007). Additionally, the Indosinian granitoids in the Xuefengshan and Yunkai-Nanling belts show similar $\varepsilon_{Nd}(t)$ values and $^{87}Sr/^{86}Sr$ ratios (Fig. 9a–c). In general, the Longtan granodiorites and granites are petrologically and geochemically similar to typical Indosinian granitoids and are considered to have been produced in a similar manner.

On the other hand, the late Indosinian Longtan granodiorites and granites and other granitoids in the Xuefengshan belt display a more restricted range of SiO_2 contents and have slightly higher K_2O and MgO contents (Fig. 5a, b) and relatively lower Rb and Zr contents, higher $\varepsilon_{Nd}(t)$ values, a wider range of initial $^{87}Sr/^{86}Sr$ ratios and younger T_{DM} ages than early Indosinian granitoids in the Yunkai-Nanling belt and arc magmatic rocks (Figs. 9, 11b, c). In summary, decreasing of zircon U–Pb ages, T_{DM} ages, increasing of $\varepsilon_{Nd}(t)$ values and variation of major and trace elements compositions define a northward trend from the Yunkai-Nanling belt to the Xuefengshan belt. This northward trend indicates a north ward tectonic process and a little older Proterozoic basement in a shallower depth of crustal remelting for the early Indosinian granitoids than the Longtan and other late Indosinian granitoids in the orogenic belt.

Previous tectonomagmatic models of plate subduction/collision within or around the SCB do not clearly explain the time–space pattern of the Indosinian granitoids and have been challenged (Wang et al. 2005a, 2007; Li and Li 2007; Carter and Clift 2008). We propose that decompressional partial melting triggered by syncollisional extension is responsible for the origin, time–space pattern and termination of Indosinian magmatism. This syncollisional extension model highlights extension, decompression and partial melting of continental crust in a collisional setting, which is analogous to the east–west extension in Himalayan orogen (Aoya et al. 2005).

Initiation of Indosinian subduction of Indochina beneath the SCB is recorded by the 267–262 Ma magmatic arc in Hainan Island (Li et al. 2006), and then plate convergence led to collision along the Song Ma suture zone at 258–243 Ma (Lepvrier et al. 1997; Carter et al. 2001; Maluski et al. 2005; Peng et al. 2006; Wang et al. 2010). A partially molten zone might have been produced in thickened middle/lower continental crust in response to progressive migration of compression (Wang et al. 2002, 2007; Ding et al. 2005; Sun et al. 2005; Shu et al. 2006; Langille et al. 2010). The <7 % low-melt fractions may have triggered a significant drop in strength of partially molten rocks (Rosenberg and Handy 2005; Le Pape et al. 2012) and a transition from compression to extension, further promoting partial melting. Middle Triassic extension, which is recorded by the Dulong-Song Chay dome and A-type

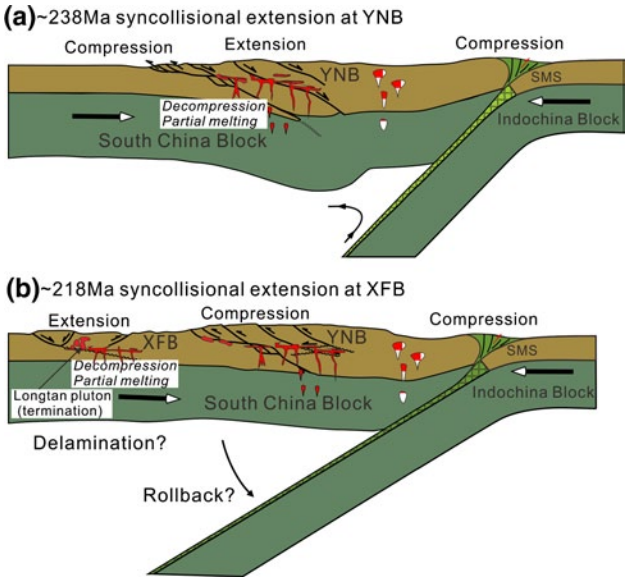

Fig. 12 A proposed tectonic model of syncollisional extension for the origin of Indosinian granitoids. **a** Early Indosinian granitoids with age peak of ~238 Ma were generated by decompressional partial melting during Middle Triassic transition from compression to extension at the Yunkai-Nanling belt. **b** Late Indosinian granitoids with age peak of ~218 Ma were derived by decompressional partial melting during Late Triassic transition from compression to extension resulted at the Xuefengshan belt, indicating termination of Indosinian Orogeny. *YNB* Yunkai-Nanling belt; *XFB* Xuefengshan belt; *SMS* Song Ma suture zone

granites (Zhao et al. 2013a, b), occur in the Yunkai-Nanling belt (Fig. 1b; Lin et al. 2008). This extension is constrained at ~238 Ma (Yan et al. 2006), consistent with the production of the early Indosinian granitoids with age peak of ~238 Ma in the Yunkai-Nanling belt (Charoy and Barbey 2008) (Fig. 12a). Meanwhile, the Xuefengshan belt moved northward along a crustal basal detachment (Wang et al. 2005b; Zhang et al. 2009). Evidence for a Late Triassic transition from compression to extension at this belt includes the N–S extensional Wugongshan dome (Fig. 1b; Faure et al. 1996; Wang et al. 2001; Liang and Li 2005). This extension triggered genesis of late Indosinian granitoids with age peak of ~218 Ma (e.g., the Longtan pluton) by decompressional partial melting of mid- to lower-level crust in the Xuefengshan belt (Le Pape et al. 2012) (Fig. 12b). These granitoid intrusions were probably produced by heating and strength drop of decompression (Peng et al. 1996; Rosenberg and Handy 2000, 2005; Brown 2007; Whittington et al. 2009). The effective vertical mass and heat transfer through diapirism produce granitoids. Such an efficient heat and mass transfer halts the flow of orogenic crust and marks the end of Indosinian orogeny (Teyssier et al. 2005). Additionally, as two possible mechanisms for such decompression, slab rollback or/and delamination, are seemingly compatible with the geologic observations (Wells et al. 2012).

Conclusions

1. The Longtan pluton in the Xuefengshan belt is composed of high-K and calc-alkaline granodiorites and granites, emplaced at 218 Ma.
2. The granodiorites were derived from partial melting of interlayed Proterozoic metabasaltic to metatonalitic source rocks, whereas the granites were derived from a mixture of Proterozoic metagraywackes and metaigneous source rocks. Geochemical evidence indicates that partial melting and fractional crystallization were dominant mechanism of the granitoid evolution.
3. The early and late Indosinian magmatic episodes with peak ages of ~238 Ma and ~218 Ma in the SCB, formed in a similar manner as Longtan granitoids, were derived from decompressional partial melting which triggered by syncollisional extension. The 218 Ma Longtan pluton marks the termination of Indosinian magmatism and orogeny in the region.

Acknowledgments This study was supported by the National Basic Program of China (2014CB440903), the NSFC (Projects 41172191 and 41372212), the CSC (201206400041), the Oversea Famous Professor Program to Nicholas Arndt (MS2011ZGDZ (BJ) 019) and State Key Laboratory of Geological Processes and Mineral Resources (GPMR2011). We thank Dr. Jianfeng Gao for assistance on the major and trace element analysis, Prof. Xianhua Li for supervision on SIMS zircon U–Pb analysis and Prof. Zhidan Zhao for help on the interpretation of Sr–Nd isotopic data. We have benefited from helpful discussions with Prof. Yu Wang, Drs. Ying Tong, Weihua Sun and Sun Tao, Miss Lu Song and Mr. Wang Junzhi during the study, and from language polishing of an early draft by Ms. Lixian Tian. We appreciate discussions and constructive comments on the manuscript by Profs. Michael L. Wells, Paul T. Robinson, Christian Dullo, Wen-Jiao Xiao, Jun-Hong Zhao and W.J. Collins.

References

Altherr R, Holl A, Hegner E, Langer C, Kreuzer H (2000) High-potassium, calc-alkaline I-type plutonism in the European variscides: northern Vosges (France) and northern Schwarzwald (Germany). Lithos 50:51–73

Annen C, Blundy JD, Sparks RSJ (2006) The genesis of intermediate and silicic magmas in deep crustal hot zones. J Petrol 47:505–539

Aoya M, Wallis SR, Terada K, Lee J, Kawakami T, Wang Y, Heizler M (2005) North–south extension in the Tibetan crust triggered by granite emplacement. Geology 33:853–856

BGMRGX (Bureau of Geology and Mineral Resources of Guangxi Zhuang Autonomous Region) (1985) Regional Geology of the Guangxi Zhuang Autonomous Region. Geological Publishing House, Beijing (in Chinese with English abstract)

BGMRHN (Bureau of Geology and Mineral Resources of Hunan Province) (1988) Regional geology of Hunan province. Geological Publishing House, Beijing (in Chinese with English abstract)

BGMRHN (Bureau of Geology and Mineral Resources of Hunan Province) (1995a) Geological maps of granitic plutons in Hunan Province. Hunan Geol 8:1–73 (in Chinese)

BGMRHN (Bureau of Geology and Mineral Resources of Hunan Province) (1995b) Distinguishing of unit-petrologic unit of granites in Hunan Province and mineralization. Hunan Geol 8:1–84 (in Chinese)

BGMRJX (Bureau of Geology and Mineral Resources of Jiangxi Province), (1984) Regional geology of the Jiangxi Province. Geological Publishing House, Beijing (in Chinese with English abstract)

Brown M (2007) Crustal melting and melt extraction, ascent and emplacement in orogens: mechanisms and consequences. J Geol Soc Lond 164:709–739

Brown M (2013) Granite: from genesis to emplacement. Geol Soc Am Bull 125:1079–1113

Carter A, Clift PD (2008) Was the Indosinian orogeny a Triassic mountain building or thermotectonic reactivation event? Comptes Rendus Geosci 340:83–93

Carter A, Roques D, Bristow C, Kinny P (2001) Understanding Mesozoic accretion in Southeast Asia: significance of Triassic thermotectonism (Indosinian orogeny) in Vietnam. Geology 29:211–214

Chappell BW (1999) Aluminium saturation in I- and S-type granites and the characterization of fractionated haplogranites. Lithos 46:535–551

Chappell BW, White AJR (1992) I- and S-type granites in the Lachlan Fold Belt. Trans R Soc Edinb Earth Sci 83:1–26

Charoy B, Barbey P (2008) Ferromagnesian silicate association in S-type granites: the Darongshan granitic complex (Guangxi, South China). Bull Geol Soc Fr 179:13–27

Charvet J (2013) The neoproterozoic-early Paleozoic tectonic evolution of the South China block: an overview. J Asian Earth Sci 74:198–209

Charvet J, Shu LS, Shi YS, Guo LZ, Faure M (1996) The building of south China: collision of Yangzi and Cathaysia blocks, problems and tentative answers. J Southeast Asian Earth Sci 13:223–235

Chauvel C, Arndt NT, Kielinczuk S, Thom A (1987) Formation of Canadian 19 Ga old continental crust I: Nd isotopic data. Can J Earth Sci 24:396–406

Chen JF, Jahn BM (1998) Crustal evolution of southeastern China: Nd and Sr isotopic evidence. Tectonophysics 284:101–133

Chen TY, Wang XY, Ren JX, Liu ZG (1986) Isotopic geochronology of the Jiuyishan and Baimashan composite granitic intrusions, Hunan. Geol Rev 32:433–439 (in Chinese with English abstract)

Chen DF, Li XH, Pang JM, Dong WQ, Chen GQ, Chen XP (1998) Metamorphic newly producted zircon, SHRIMP ion microprobe U–Pb age of amphibolite of Hexi Group, Zhejiang and its implication. Acta Miner Sin 18:396–400

Chen WF, Chen PR, Huang HY, Ding X, Sun T (2007) Chronological and geochemical studies of granite and enclave in Baimashan pluton, Hunan, South China. Sci China (D) 50:1606–1627

Chen CH, Hsieh PS, Lee CY, Zhou HW (2011) Two episodes of the Indosinian thermal event on the South China block: constraints from LA-ICPMS U–Pb zircon and electron microprobe monazite ages of the Darongshan S-type granite suite. Gondwana Res 19:1008–1023

Chen Z, Lin W, Faure M, Lepvrier C, Van Vuong N, Van Tich V (2013) Geochronology and isotope analysis of the Late Paleozoic to Mesozoic granitoids from Northeastern Vietnam and implications for the evolution of the South China block. J Asian Earth Sci. doi:10.1016/j.jseaes.2013.07.039

Cho DL, Lee SR, Armstrong R (2008) Termination of the Permo-Triassic Songrim (Indosinian) orogeny in the Ogcheon belt, South Korea: occurrence of ca. 220 Ma post-orogenic alkali granites and their tectonic implications. Lithos 105:191–200

Chu Y, Faure M, Lin W, Wang QC, Ji WB (2012a) Tectonics of the middle Triassic intracontinental Xuefengshan Belt, South China: new insights from structural and chronological constraints on the basal décollement zone. Int J Earth Sci 101:2125–2150

Chu Y, Faure M, Lin W, Wang QC (2012b) Early Mesozoic tectonics of the South China block: insights from the Xuefengshan intracontinental orogen. J Asian Earth Sci 61:199–220

Collins WJ, Beams SD, White AJR, Chappell BW (1982) Nature and origin A type granites with particular reference to Southeastern Australia. Contrib Mineral Petrol 80:189–200

Conrad CP, Bianco TA, Eugene IS, Paul W (2011) Patterns of intraplate volcanism controlled by asthenospheric shear. Nat Geosci 4:317–321

Deng XG, Chen ZG, Li XH (2004) SHRIMP U–Pb zircon dating of the Darongshan-Shiwandashan. Geol Rev 50:426–432 (in Chinese with English abstract)

Deprat J (1914) Etude des plissements et des zones décrasement de lamoyenne et de la basse RivièreNoire. Mémoire du Service Géologique Indochine 3:1–59

Ding X, Chen PR, Chen WF, Huang HY, Zhou XM (2005) LA-ICPMS zircon dating of Weishan granitic plutons in Hunan Province: petrogenesis and tectonic implications. Sci China (D) 35:606–616

Dostal J, Chatterjee AK (2000) Contrasting behaviour of Nb/Ta and Zr/Hf ratios in a peraluminous granitic pluton_Nova Scotia, Canada. Chem Geol 163:207–218

England PC, Thompson A (1986) Some thermal and tectonic models for crustal melting in continental collision zones. J Geol Soc London 19:83–94

Fan PF (2000) Accreted terranes and mineral deposits of Indochina. J Asian Earth Sci 18:343–350

Faure M, Sun Y, Shu L, Monie P, Charvet J (1996) Extensional tectonics within a subduction-type orogen-the case study of the Wugongshan dome (Jiangxi province, southeastern China). Tectonophysics 263:77–106

Faure M, Lepvrier C, Van Vuong N, Lin W, Chen Z (2013) The South China block-Indochina collision: where, when, and how? J Asian Earth Sci (in press)

Fromaget J (1927) Études géologiques sur le Nord de l'Indochine centrale. Bulletin du Service GeÂologique de l'Indochine 16:1–368

Fromaget J (1932) Sur la structure des Indosinides. Comptes Rendus de l'Académie des Sciences 195:1–538

Fromaget J (1941) L'Indochine française, sa structure geologique, ses roches, ses mines et leurs relations possibles avec la tectonique. Bulletin du Service GeÂologique de l'Indochine 26:1–140

Gardien V, Thompson AB, Grujic D, Ulmer P (1995) Experimental melting of biotite + plagioclase + quartz + muscovite assemblages and implications for crustal melting. J Geophys Res 100:15581–15591

Ge XY (2003) Mesozoic magmatism in Hainan island (SE China) and its tectonic implications: geochronology, geochemical and Sr–Nd isotope evidences. Dissertation, Guangzhou Institute of Geochemistry, Chinese Academy of Sciences

Harris NBW, Inger S (1992) Trace element modelling of pelite derived granites. Contrib Mineral Petrol 110:46–56

Harris N, Ayres M, Massey J (1995) Geochemistry of granitic melts produced during the incongruent melting of muscovite-implications for the extraction of Himalayan leucogranite magmas. J Geophys Res 100:15767–15777

Hildreth W, Moorbath S (1988) Crustal contributions to arc magmatism in the Andes of Central Chile. Contrib Mineral Petrol 98:455–489

Huang JQ, Ren JS, Jiang CF, Zhang ZK, Qin DY (1987) Geotectonic evolution of China. Springer, Berlin

Hutchison CS (1975) Ophiolites in Southeast Asia. GSA Bull 86:797–806

Inger S, Harris NBW (1993) Geochemical constraints on leucogranite magmatism in the Langtang Valley, Nepal Himalaya. J Petrol 34:345–368

Jung S, Hoernes S, Mezger K (2000) Geochronology and petrogenesis of Pan-African, syn-tectonic, S-type and post-tectonic A-type granite (Namibia): products of melting of crustal sources, fractional crystallization and wall rock entrainment. Lithos 50:259–287

Kalsbeek F, Jepsen HF, Nutman AP (2001) From source migmatites to plutons: tracking the origin of ca 435 Ma S-type granites in the East Greenland Caledonian Orogen. Lithos 57:1–21

Kemp AIS, Whitehouse MJ, Hawkesworth CJ, Alarcon MK (2005) A zircon U-Pb study of metaluminous (I-type) granites of the Lachlan Fold Belt, southeastern Australia: Implications for the high/low temperature classification and magma differentiation processes. Contrib Mineral Petrol 150:230–249

Koester E, Pawley AR, Luĩ AD, Fernandes LAD, Porcher CC, Soliani E Jr (2002) Experimental melting of cordierite gneiss and the petrogenesis of syntranscurrent peraluminous granites in Southern Brazil. J Petrol 43:1595–1616

Lacassin R, Leloup H, Trinh V, Tapponnier P (1998) Unconformity of red sandstones in North Vietnam: field evidence for Indosinian orogeny in northern Indochina? Terra Nova 10:106–111

Lai SC, Zhang GW, Li SZ (2004) Ophiolites from the Mianlüe Suture in the southern Qinling and their relationship with the eastern Paleotethys evolution. Acta Geol Sin 78:107–117

Langille J, Lee J, Hacker B, Seward G (2010) Middle crustal ductile deformation patterns in southern Tibet: insights from vorticity studies in Mabja Dome. J Struct Geol 32:70–85

Le Maitre RW (2002) Igneous rocks: a classification and glossary of terms. Cambridge University Press, Cambridge

Le Pape F, Jones AG, Vozar J, Wenbo W (2012) Penetration of crustal melt beyond the Kunlun fault into northern Tibet. Nature Geosci 5:330–335

Lepvrier C, Maluski H, Van Vuong N, Rogues D, Axente V, Rangin C (1997) Indosinian NW-trending shear zones within the Truong Son belt (Vietnam) ^{40}Ar–^{39}Ar Triassic ages and Cretaceous to Cenozoic overprints. Tectonophysics 283:105–127

Lepvrier C, Maluski H, Tich VV, Leyreloup A, Thi PT, Vuong NV (2004) The early Triassic Indosinian orogeny in Vietnam (Truong Son Belt and Kontum Massif): implications for the geodynamic evolution of Indochina. Tectonophysics 393:87–118

Lepvrier C, Vuong NV, Maluski H, Thi PT, Vu TV (2008) Indosinian tectonics in Vietnam. Comptes Rendus Geosci 340:94–111

Li XH (1994) A compressive U-Pb, Sm–Nd, Rb–Sr and ^{40}Ar–^{39}Ar geochronological study on Guidong granodiorite, southeast China: records of multiple tectonothermal events in a single pluton. Chem Geol 115:283–295

Li XH, Li ZX, Li WX, Wang YJ (2006) Initiation of the Indosinian Orogeny in South China: evidence for a Permian magmatic arc on the Hainan Island. J Geol 114:341–353

Li XH, Liu Y, Li QL, Guo CH, Chamberlain KR (2009) Precise determination of Phanerozoic zircon Pb/Pb age by multi-collector SIMS without external standardization. Geochem Geophys Geosyst 10:Q04010

Li XH, Li WX, Li QL, Wang XC, Liu Y, Yang YH (2010) Petrogenesis and tectonic significance of the ~850 Ma Gangbian alkaline complex in South China: evidence from in situ zircon U–Pb dating, Hf–O isotopes and whole-rock geochemistry. Lithos 114:1–15

Li ZX, Li XH (2007) Formation of the 1300-km-wide intracontinental orogen and postorogenic magmatic province in Mesozoic South China: a flat-slab subduction model. Geology 35:179–182

Liang XQ, Li XH (2005) Late Permian to Middle Triassic sedimentary records in Shiwandashan basin: implication for the Indosinian Yunkai Orogenic Belt, South China sedimentary. Geology 177:297–320

Lin W, Wang Q, Chen K (2008) Phanerozoic tectonics of south China block: new insights from the polyphase deformation in the Yunkai massif. Tectonics 27(TC6004):1010

Ludwig KR (2003) ISOPLOT 30: a geochronological toolkit for microsoft excel, Berkeley Geochronology Center. Special Publ 51:507–513

Maluski H, Lepvrierb C, Leyreloup A, Tich VV, Thi PT (2005) ^{40}Ar–^{39}Ar geochronology of the charnockites and granulites of the Kan Nack complex, Kon Tum Massif, Vietnam. J Asian Earth Sci 25:653–677

Mao J, Takahashi Y, Kee WS, Li Z, Ye H, Zhao X, Liu K, Zhou J (2011) Characteristics and geodynamic evolution of Indosinian magmatism in South China: a case study of the Guikeng pluton. Lithos 127:535–551

Mattinson JM (2005) Zircon U–Pb chemical abrasion (''CA-TIMS'') method: combined annealing and multi-step partial dissolution analysis for improved precision and accuracy of zircon ages. Chem Geol 220:47–66

McDermott F, Harris NBW, Hawkesworth CJ (1996) Geochemical constraints on crustal anatexis: a case study from the Pan-African Damara granitoids of Namibia. Contrib Mineral Petrol 123:406–423

Metcalfe I (2002) Permian tectonic framework and palaeogeography of SE Asia. J Asian Earth Sci 20:551–566

Metcalfe I (2006) Palaeozoic and Mesozoic tectonic evolution and palaeogeography of East Asian crustal fragments: the Korean Peninsula in context. Gondwana Res 9:24–46

Metcalfe I (2011) Tectonic framework and Phanerozoic evolution of Sundaland. Gondwana Res 19:3–21

Middlemost EAK (1994) Naming materials in the magma/igneous rock system. Earth Sci Rev 74:193–227

Morrison GW (1980) Characteristics and tectonic setting of the shoshonite rock association. Lithos 13:97–108

Patiño Douce AE (1996) Effects of pressure and H_2O content on the composition of primary crustal melts. Trans R Soc Edinburgh: Earth Sci 87:11–21

Patiño Douce AE, Beard JS (1995) Dehydration-melting of biotite gneiss and quartz amphibolite from 3 to 15 kbar. J Petrol 36:707–738

Patiño Douce AE, Beard JS (1996) Effects of P, f (O_2) and Mg/Fe ratio on dehydration melting of model metagreywackes. J Petrol 37:999–1024

Peng SM, Fu LF, Zhou GQ (1996) Tectonic Evolution of Yunkai Massif and its Shearing Anatectic Origin of Gneissic Granitic Rocks. China University of Geosciences Press, Wuhan (in Chinese with English abstract)

Peng TP, Wang YJ, Fan WM, Liu DY, Shi YR, Miao LC (2006) The SHRIMP zircon U–Pb geochronology of the early Mesozoic felsic igneous rocks from the southern Lancangjiang and its tectonic implications. Sci China (D) 49:1032–1042

Petford N, Cruden AR, McCaffrey KJW, Vigneresse JL (2000) Granite magma formation, transport and emplacement in the earth's crust. Nature 408:669–673

Qi L, Hu J, Greggoire C (2000) Determination of trace elements in granites by inductively coupled plasma mass spectrometry. Talanta 51:507–513

Qi CS, Deng XG, Li XH, Li WX, Yang YH, Xie LW (2007) Origin of the Darongshan-Shiwandashan S-type granitoid belt from southeastern Guangxi: geochemical and Sr–Nd–Hf isotopic constraints. Acta Petrol Sin 23:403–412

Qiu JT, Song WJ, Jiang CX, Wu H, Dong MR (2013) CGDK: an extensible CorelDRAW VBA program for geological drafting. Comput Geosci 51:34–48

Ratschbacher L, Hacker BR, Calvert A, Webb LE, Grimmer JC, McWilliams MO, Ireland T, Dong SW, Hu JM (2003) Tectonics

of the Qinling (central China): tectonostratigraphy, geochronology, and deformation history. Tectonophysics 366:1–53

Ren JS (1996) The continental tectonic of China. J Asian Earth Sci 13:197–204

Roberts MP, Clemens JD (1993) Origin of high-potassium, calc-alkaline, I-type granitoids. Geology 21:825–828

Rosenberg CL, Handy MR (2000) Syntectonic melt pathways during simple shearing of a partially molten rock analogue (Norcamphor–Benzamide). J Geophys Res 105:3135–3149

Rosenberg CL, Handy MR (2005) Experimental deformation of partially melted granite revisited: implications for the continental crust. J Metamorph Geol 23:19–28

Schilling FR, Partzsch GM, Brasse H, Schwarz G (1997) Partial melting below the magmatic arc in the central Andes deduced from geoelectromagnetic field experiments and laboratory data. Phys Earth Planet Inter 103:17–31

Schmitz M, Heinsohn WD, Schilling FR (1997) Seismic, gravity and petrological evidence for partial melt beneath the thickened Central Andean crust. Tectonophysics 270:313–326

Shen WZ, Zhu JC, Liu CS, Xu SJ, Ling HF (1993) Sm–Nd isotopic study of basement metamorphic rocks in south China and its constraint on material sources of granitoids. Acta Petrol Sin 9:115–124 (in Chinese with English abstract)

Shen WZ, Ling HF, Li WX, Wang DZ (1998) Sr and Nd isotope of Mesozoic granitoids in Jiangxi Province. Chin Sci Bull 43:2653–2657

Shu LS, Zhou XM, Deng P, Yu XQ (2006) Principal geological features of Nanling Tectonic Belt, South China. Geol Rev 52:251–265 (in Chinese with English abstract)

Shu LS, Faure M, Wang B, Zhou XM, Song B (2008) Late Palaeozoic-early Mesozoic geological features of South China: response to the Indosinian collision events in Southeast Asia. Comptes Rendus Geosci 340:151–165

Simpson RL, Parrish RR, Searle MP, Waters DJ (2000) Two episodes of monazite crystallization during metamorphism and crustal melting in the Everest region of the Nepalese Himalaya. Geology 28:403–406

Sun SS, McDonough WF (1989) Chemical and isotopic systematics of oceanic basalts: implications for mantle composition and processes In: Saunders, AD, Norry, MJ (eds) Magmatism in the ocean basins. J Geol Soci London, pp 313–345

Sun T, Zhou XM, Chen PR, Li HM, Zhou HY, Wang ZC, Shen WZ (2005) Strongly peraluminous granites of Mesozoic in Eastern Nanling range, southern China: petrogenesis and implications for tectonics. Sci China (D) 48:165–174

Sylvester PJ (1998) Postcollisional strongly peraluminous granites. Lithos 45:29–44

Taylor SR, McLennan SM (1985) The continental crust: its composition and evolution. Oxford Press/Blackwell, Oxford

Teyssier C, Ferre E, Whitney DL, Norlander B, Vanderhaeghe O, Parkinson D (2005) Flow of partially molten crust and origin of detachments during collapse of the Cordilleran Orogen. J Geol Soc Lond 245:39–64

Thompson AB (1996) Fertility of crustal rocks during anatexis. Trans R Soc Edinburgh: Earth Sci 87:1–10

Trung NM, Tsujimori T, Itaya T (2006) Honvang serpentinite body of the Song Ma fault zone, Northern Vietnam: a remnant of oceanic lithosphere within the Indochina-South China suture. Gondwana Res 9:225–230

Vanderhaeghe O, Teyssier C (2001) Partial melting of crust and flow of orogens. Tectonophysics 342:451–472

Vielzeuf D, Schmidt NW (2001) Melting relations in hydrous systems revisited: application to metapelites, metagreywackes and metabasalts. Contrib Mineral Petrol 141:251–267

Wan TF (2011) The tectonics of China-data, maps and evolution. Springer and Higher Education Press, Berlin and Beijing

Wan YS, Liu DY, Simon AW, Cao J, Chen B, Dong CY, Song B, Ll Du (2010) Evolution of the Yunkai Terrane, South China: evidence from SHRIMP zircon U–Pb dating, geochemistry and Nd isotope. J Asian Earth Sci 37:140–153

Wang BQ, Zhou MF, Li JW, Yan DP (2011) Late Triassic porphyritic intrusions and associated volcanic rocks from the Shangri-La region, Yidun terrane, Eastern Tibetan Plateau: adakitic magmatism and porphyry copper mineralization. Lithos 127:24–38

Wang J, Li ZX (2003) History of Neoproterozoic rift basins in South China: implications for Rodinia break-up. Precambrian Res 1–4:141–158

Wang YJ, Fan WM, Guo F, Li HM, Liang XQ (2001) U-Pb dating of early Mesozoic granodioritic intrusions in southeastern Hunan Province, South China and its petrogenetic implications. Sci China (D) 31:745–751 (in Chinese)

Wang YJ, Zhang YH, Fan WM, Xi XW, Guo F, Lin G (2002) Numerical modeling for generation of Indosinian peraluminous granitoids Hunan Province: basaltic underplating versus tectonic thickening. Sci China (D) 45:1042–1056

Wang YJ, Fan WM, Liang XQ, Peng TP, Shi YR (2005a) SHRIMP zircon U–Pb geochronology of Indosinian granites in Hunan Province and its petrogenetic implications. Chin Sci Bull 50:1395–1403

Wang YJ, Zhang YH, Fan WM, Peng TP (2005b) Structural signatures and $^{40}Ar/^{39}Ar$ geochronology of the Indosinian Xuefengshan tectonic belt, South China block. J Struct Geol 27:985–998

Wang YJ, Fan WM, Sun M, Sun M, Liang XQ, Zhang YH, Peng PT (2007) Geochronological, geochemical and geothermal constraints on petrogenesis of the Indosinian peraluminous granites in the South China block: a case study in the Hunan Province. Lithos 96:475–502

Wang YJ, Fan W, Zhang G, Zhang Y (2013) Phanerozoic tectonics of the South China block: key observations and controversies. Gondwana Res 23:1273–1305

Wang YJ, Zhang AM, Fan WM, Peng TP, Zhang FF, Zhang YZ, Bi XW (2010) Petrogenesis of late Triassic post-collisional basaltic rocks of the Lancangjiang tectonic zone, southwest China, and tectonic implications for the evolution of the eastern Paleotethys: geochronological and geochemical constraints. Lithos 120:529–546

Wells ML, Hoisch TD, Cruz-Uribe AM, Vervoort JD (2012) Geodynamics of synconvergent extension and tectonic mode switching: constraints from the Sevier orogen. Tectonics 31:TC1002

Whalen JB, Currie KL, Chappell BW (1987) A-type granites: geochemical characteristics, discrimination and petrogenesis. Contrib Mineral Petrol 95:407–419

Whittington AG, Hofmeister AM, Nabelek PI (2009) Temperature-dependent thermal diffusivity of the earth's crust and implications for magmatism. Nature 458:319–321

Xiao WJ, He H (2005) Early Mesozoic thrust tectonics of the northwest Zhejiang region (southeast China). Geol Soc Am Bull 117:945–961

Xiao WJ, Windley BF, Yuan C, Sun M, Han CM, Lin SF, Chen HL, Yan QR, Liu DY, Qin KZ, Li JL, Sun S (2009) Paleozoic multiple subduction-accretion processes of the southern Altaids. Am J Sci 309:221–270

Xie CF, Zhu JC, Ding SJ, Zhang YM, Chen ML, Fu YR, Fu TA, Li ZH (2006) Age and petrogenesis of the Jianfengling granite and its relationship to metallogenesis of the Baolun gold deposit, Hainan Island. Acta Petrol Sin 22:2493–2508 (in Chinese with English abstract)

Xu C, Huang ZL, Qi L, Fu PQ, Liu CQ, Li ED, Guan T (2007) Geochemistry of Cretaceous granites from Mianning in the Panxi region, Sichuan Province, southwestern China: implications for their generation. J Asian Earth Sci 29:737–750

Yan DP, Zhou MF, Song HL, Wang XW, Malpas J (2003) Origin and tectonic significance of a Mesozoic multi-layer over-thrust

system within the Yangtze Block (South China). Tectonophysics 361:239–254

Yan DP, Zhou MF, Wang Y, Xia B (2006) Structural and geochronological constraints on the tectonic evolution of the Dulong-Song Chay tectonic dome in Yunnan province, SW China. J Asian Earth Sci 28:332–353

Yang JH, Peter AC, Du YS, Huang H, Hu LS (2012) Detrital record of Indosinian mountain building in SW China: provenance of the Middle Triassic turbidites in the Youjiang Basin. Tectonophysics 574–575:105–117

Yu JH, Wang LJ, Wang XL, Qiu JS, Zhao L (2007) Geochemistry and geochronology of the Fucheng complex in the southeastern Jiangxi province, China. Acta Petrol Sin 23:1441–1456 (in Chinese with English abstract)

Zhang HF, Harris N, Parrish R, Kelley S, Zhang L, Rogers N, Argles T, King J (2004a) Causes and consequences of protracted melting of the mid-crust exposed in the North Himalayan antiform. Earth Planet Sci Lett 228:195–212

Zhang WL, Hua RM, Wang RC, Li HM, Chen PR (2004b) Single zircon U–Pb isotopic age of the Wuliting granite in Dajishan area of Jiangxi and its geological implication. Acta Geol Sin 78:352–358 (in Chinese with English abstract)

Zhang XW, Xiang H, Zhong ZQ, Zhou HW, Zhang L, Yang N, Wang J (2009) U–Pb Dating and trace elements composition of hydrothermal zircons from Jianfengling granite, Hainan: restriction on the age of hydrothermal event and mineralization of Baolun gold deposit. J China Univ Geosci 34:921–930 (in Chinese with English abstract)

Zhao L, Guo F, Fan WM, Li CW, Tan XF, Li WX (2010) Crustal evolution of the Shiwandashan area in South China: zircon U–Pb–Hf isotopic records from granulite enclaves in Indo-Sinian granites. Chin Sci Bull 55:1489–1498

Zhao JH, Zhou MF, Yan DP, Zheng JP, Li JW (2011) Reappraisal of the ages of Neoproterozoic strata in South China: no connection with the Grenvillian orogeny. Geology 39:299–302

Zhao JH, Zhou MF, Zheng JP (2013a) Neoproterozoic high-K granites produced by melting of newly formed mafic crust in the Huangling region, South China. Precambrian Res 233:93–107

Zhao KD, Jiang SY, Chen WF, Chen PR, Ling HF (2013b) Zircon U–Pb chronology and elemental and Sr–Nd–Hf isotope geochemistry of two Triassic A-type granites in South China: implication for petrogenesis and Indosinian transtensional tectonism. Lithos 160–161:292–306

Zhou MF, Yan DP, Kennedy AK, Li Y, Ding J (2002) SHRIMP U–Pb zircon geochronological and geochemical evidence for Neoproterozoic, arc-magmatism along the western margin of the Yangtze block, South China. Earth Planet Sci Lett 196:51–67

Zhou XM, Sun T, Shen WZ, Shu LS, Niu YL (2006) Petrogenesis of Mesozoic granitoids and volcanic rocks in South China: a response to tectonic evolution. Episodes 29:26–33

Zhou D, Sun Z, Chen HZ, Xu HH, Wang WY, Pang X, Cai DS, Hu DK (2008) Mesozoic Paleogeography and tectonic evolution of South China Sea and adjacent areas in the context of Tethyan and Paleo-Pacific interconnections. Isl Arc 17:186–207

Zhuang JL, Liu ZW, Tan BX (1988) Relation of the small rock bodies in southern Hunan to the formation of ore deposits and prognosis of concealed deposits. Hunan Geol 4:1–163 (in Chinese)